



Tool durability and steel microstructure in friction stir welding of mild steel

A. De¹, H. K. D. H. Bhadeshia² and T. DebRoy³

¹Indian Institute of Technology Bombay, ²Cambridge University,

³The Pennsylvania State University

Abstract

A previously established scheme to assess tool durability and tool life in the friction stir welding (FSW) of difficult aluminium alloys has been applied to the FSW of steel. The calculations were extended to predict the consequences for the microstructure of the steel while optimizing tool life. This is believed to be the first published model that covers both the processing parameters and the consequences on the physical metallurgy of the steel.

This is an edited version of a paper published in Materials Science and Technology (2014, Vol. 30, pp. 1050–1056: ©2014 IOM3, reproduced with permission), The complete version including full referencing is freely available at: <http://tinyurl.com/mst-fsw>.

Tools for friction stir welding (FSW) of aluminium alloys are cost effective and durable, whereas the much larger market for welding of steels remains largely out of the reach of FSW because of the high cost and insufficient durability of current tooling. A recent review of tool materials by Rai and the present authors indicates that severe stresses and high temperatures pose a formidable challenge for the development of tools for the FSW of hard alloys.

As a result, initial commercial applications of FSW to steels are likely to be in niche areas where fusion welding has serious difficulties, provided the required structure and properties can be achieved by FSW. Improved tool durability and a metallurgical knowledge base of microstructure and properties are important prerequisites for expanding the reach of FSW to steels.

Since FSW is difficult for hard alloys, there is a dearth of information to guide selection of welding conditions. Chemical and mechanical erosion are possible mechanisms of tool degradation, but are not considered here: structural integrity is the focus and the “tool durability” referred to below does not include erosion induced degradation.

Experimental estimation of stresses and temperatures experienced by the tool pin during FSW remains a challenge because the pin is embedded within the hot plasticised-alloy. We have recently shown that the ability of a tool to endure stresses at high temperatures can be analysed using a heat transfer and material flow model for the welding of 7075 aluminium alloy. The results were presented as easy to use maps of “tool durability index” (see below). By selecting appropriate welding variables, it is often possible to avoid premature tool degradation/failure primarily due to shear. This article documents the first effort to enhance tool durability by focusing on the shear stress experienced during FSW of a mild steel.

The reported heating and the cooling rates of alloys during FSW fall within the range of values reported in fusion welding. Therefore, the phase transformations are unlikely to be significantly different if cooling rate is the only factor. However, two features distinguish the evolution of microstructure of FSW steels. First, peak temperatures for FSW are lower; as a result, the grain size of austenite that forms in the heat affected zone of FSW joints is often smaller than that for fusion welding. Second, severe flow of plasticised steel alters the stability of austenite in the thermo-mechanically affected zone in FSW.

Methodology

A. Tool durability index

During the FSW of steels, temperature and stress can be calculated from a well-tested, three-dimensional heat transfer and visco-plastic flow model. The computational model used in the present study solves the equations of conservation of mass, momentum and energy together with two sub-models to estimate local variations in heat generation rate and viscosity. The model has correctly predicted independent experimental results of thermal cycles, torque and traverse force in FSW of aluminium alloys, steels and a titanium alloy. Full details of the computational model are available in most of these previous publications.

Progressive tool degradation may be minimised by focusing on the maximum shear stress and peak temperature for various welding conditions. Vibration and other abrupt causes of tool degradation are not included for simplicity and the variations during the initial insertion or the final withdrawal are neglected. A flat shoulder geometry and a cylindrical tool pin without any thread are considered. It is important to evaluate the effects of welding conditions on tool durability before progressing toward more complex tool geometries.

Following Tresca's yield criterion, the resultant maximum shear stress, t_m , at any given location on the pin profile is obtained^{25,26} from shear stresses due to bending (t_B) and torsion (t_T) and the normal stress due to bending (s_B) as:

$$\tau_m = \sqrt{\left(\frac{\sigma_B}{2}\right)^2 + (\tau_B + \tau_T \sin\theta)^2 + (\tau_T \cos\theta)^2} \quad (1)$$

where q is the angle between the radius passing through the location and the welding direction. t_m has its highest value at $q=90^\circ$ for a pin with a circular cross-section.



The tool durability index is defined as the *ratio of the shear strength of the tool material to the maximum shear stress on the tool pin*. If t_m is much less than the shear strength of the tool material at the peak temperature, the tool is assumed to be able to endure the stress and temperature safely. Tool durability index contours are plotted to allow the effects of tool and welding parameters to be easily determined. Since pin length depends on the thickness of the workpiece, durability can be enhanced by ensuring adequate softening of the workpiece material (i.e. via a larger shoulder diameter or lower welding speed) or by increasing the strength of the pin via an effective increase in its load bearing mass.

B. Microstructure

Thermal cycles computed from the heat transfer and materials flow model are used to calculate the microstructure of the weld zone. For most welding conditions, austenite forms in the entire weld zone and its decomposition during cooling is modelled to determine the final microstructure, using a model developed by Jones and Bhadeshia and adapted later to include bainite. Simultaneous formation of phases such as allotriomorphic ferrite, Widmanstätten ferrite and pearlite, which compete for untransformed austenite, is considered. The model accounts for overlapping interaction of phases that touch each other and overlapping of concentration and temperature fields. There are sub-models for each individual phase in terms of its atomic mechanism of transformation (e.g. diffusional or paraequilibrium displacive transformation).

The solutes included are C, Mn, Si, Ni, Mo, Cr, V. The nucleation of phases and evolution of the transformed region during growth of Widmanstätten ferrite, and the associated strain energy, are considered together with partitioning of carbon to the austenite by diffusion. The method has been validated by calculating fractions of allotriomorphic ferrite, Widmanstätten ferrite and pearlite as a function of chemical composition, austenite grain size and thermal cycles. It is important to note that the program is used here without modification: there is no fitting to accommodate any difficulties in predicting structure. This is because the method has been extensively validated for wrought steels, so if there are any peculiarities of FSW then they should be revealed by applying an unadulterated calculation.

To repeat: the model used here is radically different from that for welds that involve fusion, where the structure evolves from the liquid state. For FSW, it is appropriate to use a method based on evolution of structure in the solid-state. As will be seen, there are complications because some parts of the FSW joint exist in a plastically deformed state prior to the transformation of austenite, a phenomenon that has not been considered at all in the descriptions of structure of such welds, but is well established in other scenarios involving wrought steels.

Results

Figure 1 shows that the calculated peak temperatures for 1018 steel under FSW at 0.42 mm/s and a tool rotational speed of 450 rpm at the top plane are somewhat (~150°C) higher than that at the bottom plane.

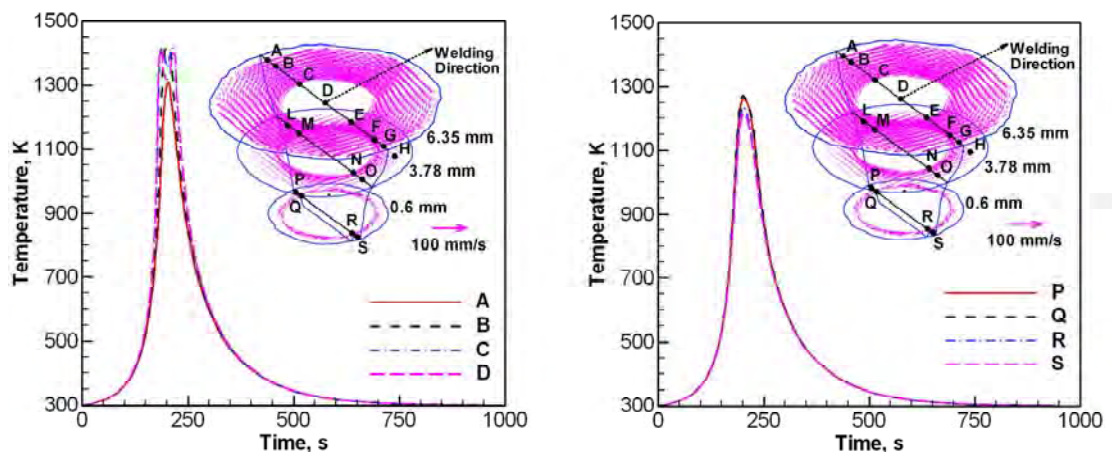


Figure 1

However, the cooling rates did not change significantly at various locations.

Data used for the calculations are presented in Table 1 of the full paper where it is shown that cooling rates change significantly with welding speed at all the monitoring locations. In contrast, the cooling rate did not change significantly with the rotational speed, although the temperatures are somewhat higher near the shoulder at higher tool rotational speeds. This finding is consistent with independent observations³⁶ of FSW of HSLA 65 steel.

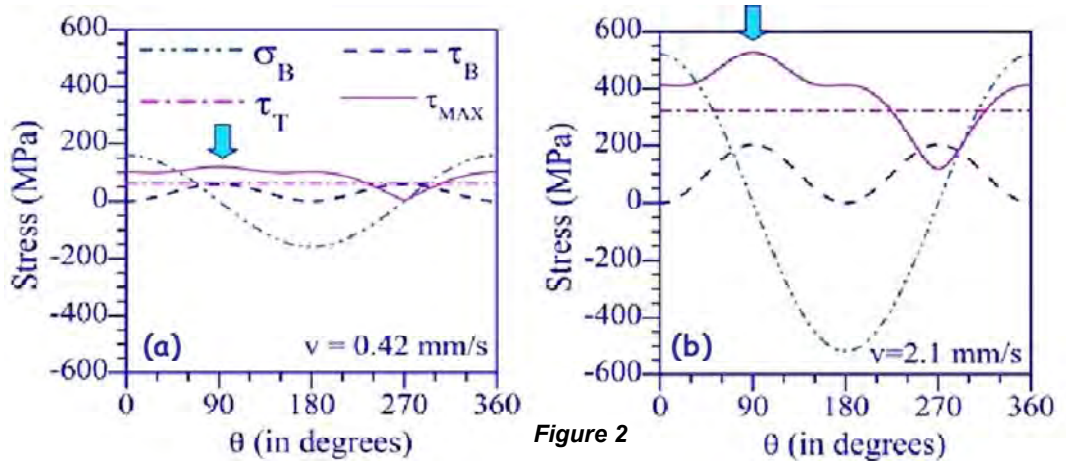
The microstructure calculations were performed at a tool rotational speed of 300 rpm and welding speed of 0.42 mm/s, for the region next to the pin at the top and middle horizontal planes, where the cooling rates were in the range of 20 and 8°C/s. Our calculations for the appropriate chemical composition (Fe-0.18C-0.82Mn), cooling rate and austenite grain size did not generate the microstructures reported by Lienert et al. for the stir zone (*Weld. J.*, 2003, **82**, (1), 1s-9s). It is not possible from the two micrographs available in that study, to make more than a rough estimate of the phases obtained in the centre of the stir zone and at the top of that zone, but these are quite different from the calculations, which show very little transformation during cooling at the rates expected in the two regions of the stir zone (see Table 2 of the full paper). Unlike in fusion welds, the stir zone is thermo-mechanically processed prior to transformation. Such processing introduces defects in the austenite, which then contribute to the chemical free energy change for phase transformation at elevated temperatures.

Introducing what is considered a conservative value of 200 J mol⁻¹ for the stored energy due to deformation (with reference to studies of hot rolling of mild steels) into the calculation produces a dramatic effect on the microstructural evolution, which is now more consistent with the observed structures.

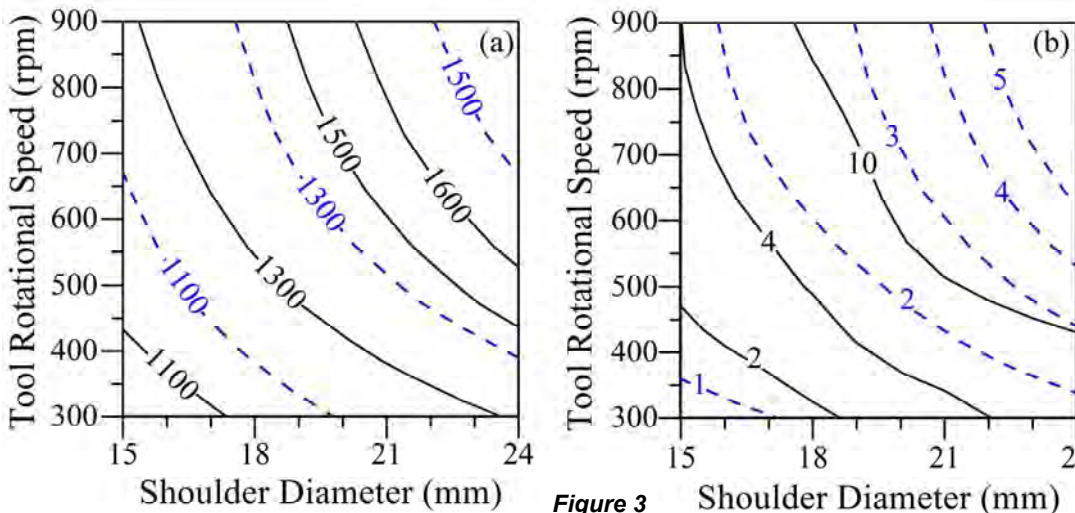
Continued page 6



Figure 2 shows the typical variation of various stresses during one rotation of the tool pin as a function of the orientation angle (θ) with the welding direction for two welding speeds at 450rpm. The resultant maximum shear stress is influenced primarily by the shear stresses due to bending and torsion, and attains the maximum at $\theta = 90^\circ$. Both the magnitude and fluctuation of the resultant maximum shear stress increase significantly with increasing welding speed. Increasing the welding speed reduces the heat input per unit length resulting in lower peak temperature, higher traverse force and higher stresses on the pin.



Maps have been produced for peak temperature and tool durability index as a function of shoulder diameter and rotational speed for the FSW of C-Mn 1018 steel, to demonstrate the effect of welding speed, plate thickness and pin diameter. An increase in welding speed reduces the rate of heat generation per unit length of weld resulting in relatively cool, hard material around the tool pin (**Figure 3**) where the solid and broken lines represent welding speeds of



1.05 and 2.1 mm/s respectively.

As a result, the stresses on the tool increase because the workpiece material becomes harder and consequently, the tool durability index decreases with increase in welding speed.

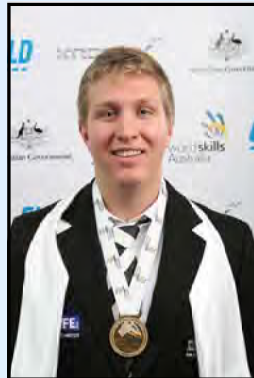
During FSW of thick plates, there is considerable decrease in temperature away from the tool shoulder and the lower part of the pin encounters cooler and stronger workpiece. The tool encounters larger stresses and the tool durability index decreases with increasing plate thickness. An increase in pin diameter increases the rate of heat generation per unit length of weld, resulting in an increase of the peak temperature. As a result, the stresses on the tool decrease because the workpiece material becomes softer and tool durability index increases with increasing pin diameter.

Summary

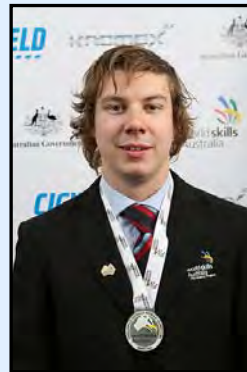
In the 800–500°C temperature range, the cooling rates in FSW are significantly affected by the welding speed but not by the tool rotational speed. It has been demonstrated that the microstructure of the weld zone during FSW of 1018 steel can be estimated if account is taken of the deformation of the austenite prior to its transformation. This is quite unlike fusion welds where the austenite is essentially free from defects. However, the calculations highlight a need for the better quantitative characterisation of the microstructural constituents of the stir zone of friction stir welds in steels. Furthermore, this needs to be done as a function of position in the stir zone. Computational models are in this sense more advanced than experimental data, since the stored energy gradients within the stir zone can in principle be calculated.

For the FSW of mild steel, an increase in either the tool shoulder diameter or the tool rotational speed increase workpiece temperature and hence, enhances tool durability. A faster welding speed reduces peak temperature, increases stresses on the tool and thus, reduces tool durability. Thicker plates also decrease tool durability for the same reasons. In contrast, thicker tool pins increase tool durability because of enhanced structural stiffness.

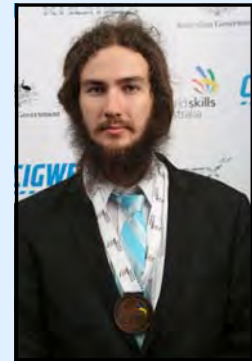
WorldSkills Perth 2014 Success



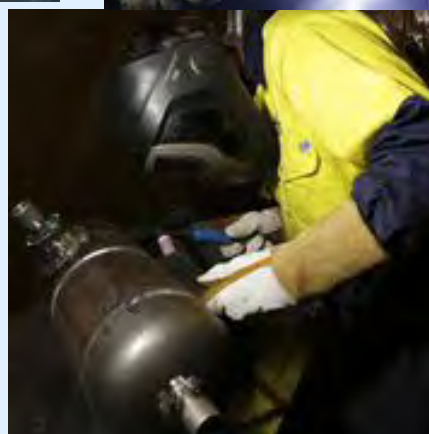
GOLD: Kallon McVicar,
Illawarra - NSW



SILVER: Nathan Kelly,
Macquarie - NSW



BRONZE: Elton Stewart-Murray,
Tasmania



The Welding competitors were required to complete a series of test plates and pipes, assemble and weld a complex carbon steel pressure vessel and also complete stainless steel and aluminium projects. These tasks involved using tig, stick, mig and flux-core welding procedures which are all marked to industry standards.

About WorldSkills continued page 2